N-Type Conjugated Polymer-Enabled Selective Dispersion of Semiconducting Carbon Nanotubes for Flexible CMOS-Like Circuits

*Huiliang Wang, Yaoxuan Li, Gonzalo Jiménez-Osés, Peng Liu, Ya Fang, Jie Zhang, Ying-Chih Lai, Steve Park, Liwei Chen, Kendall N. Houk, and Zhenan Bao**

Sorting of semiconducting single-walled carbon nanotubes (SWNTs) by conjugated polymers has attracted considerable attention recently because of its simplicity, high selectivity, and high yield. However, up to now, all the conjugated polymers used for SWNT sorting are electron-donating (p-type). Here, a high-mobility electron-accepting (n-type) polymer poly([N,N′-bis(2-octyldodecyl)-naphthalene-1,4,5,8-bis(dicarboximide)-2,6-diyl]-alt-5,5′-(2,2′-bithiophene)) (P(NDI2OD-T2)) is utilized for the sorting of high-purity semiconducting SWNTs, as characterized by Raman spectroscopy, dielectric force spectroscopy and transistor measurements. In addition, the SWNTs sorted by P(NDI2OD-T2) have larger diameters than poly(3-dodecylthiophene) (P3DDT)-sorted SWNTs. Molecular dynamics simulations in explicit toluene demonstrate distinct linear or helical wrapping geometry between P(NDI2OD-T2) and different types of SWNTs, likely as a result of the strong interactions between the large aromatic core of the P(NDI2OD-T2) backbone and the hexagon path of SWNTs. By using high-mobility n-type P(NDI2OD-T2) as the sorting polymer, ambipolar SWNT transistors with better electron transport than that attained by P3DDT-sorted SWNTs are achieved. As a result, flexible negated AND and negated OR logic circuits from the same set of ambipolar transistors are fabricated, without the need for doping. The use of n-type polymers for sorting semiconducting SWNTs and achieving ambipolar SWNT transistor characteristics greatly simplifies the fabrication of flexible complementary metal-oxide-semiconductor-like SWNT logic circuits.

1. Introduction

Single-walled carbon nanotubes (SWNTs) have been widely studied for applications in flexible electronics due to their high charge carrier mobilities,[1] mechanical flexibility/stretchability,[2,3] and compatibility with printed electronics.[4] However, as-synthesized SWNTs are mixtures of semiconducting SWNTs (s-SWNTs) and metallic SWNTs (m-SWNTs), hindering their practical deployment in semiconductor-based electronics. Hence, a major focus of research in the area of SWNT electronics has been on sorting and isolating s-SWNTs. Methods used have included density gradient centrifugation,[5] sorting by DNAs,[6] gel chromatography,[7] partition separation,[8] and selective dispersion by conjugated polymers.[9] Sorting of SWNTs by conjugated polymers is of particular interest because of its simplicity, high selectivity, and high yield.[9–12]

Although a significant progress has been made on the sorting of semiconducting SWNTs by various conjugated polymers,[9–11,13,14] the mechanism of sorting is still under investigation. One possibility is that sorting is a result of stronger charge transfer between polymers and more polarizable m-SWNTs.[11,15] In particular, several reports have also shown that electron acceptor molecules interact more favorably with m-SWNTs through charge transfer.[16] To date, the polymers used for sorting SWNTs have all been electron-donating (p-type) polymers with shallow LUMO levels. Therefore, one might also expect that acceptor (n-type) polymers may interact more strongly than p-type polymers with m-SWNTs due to their deeper LUMO levels.

H. Wang, Y. Li, Y. Fang, Y.-C. Lai, S. Park, Prof. Z. Bao
Department of Materials Science and Engineering
Department of Electrical Engineering
and Department of Chemical Engineering
Stanford University
Stanford, CA 94305, USA
E-mail: zbao@stanford.edu

Dr. G. Jiménez-Osés, Dr. P. Liu, Prof. K. N. Houk
Department of Chemistry and Biochemistry
University of California
Los Angeles, CA 90095, USA

J. Zhang, L. Chen
i-Lab, Suzhou Institute of Nano-Tech and Nano-Bionics
Chinese Academy of Sciences
Suzhou, Jiangsu 215125, China

Y.-C. Lai
Graduate Institute of Electronics Engineering
National Taiwan University
Taipei 106, Taiwan, Republic of China

DOI: 10.1002/adfm.201404126

© 2015 WILEY-VCH Verlag GmbH & Co. KGaA, Weinheim

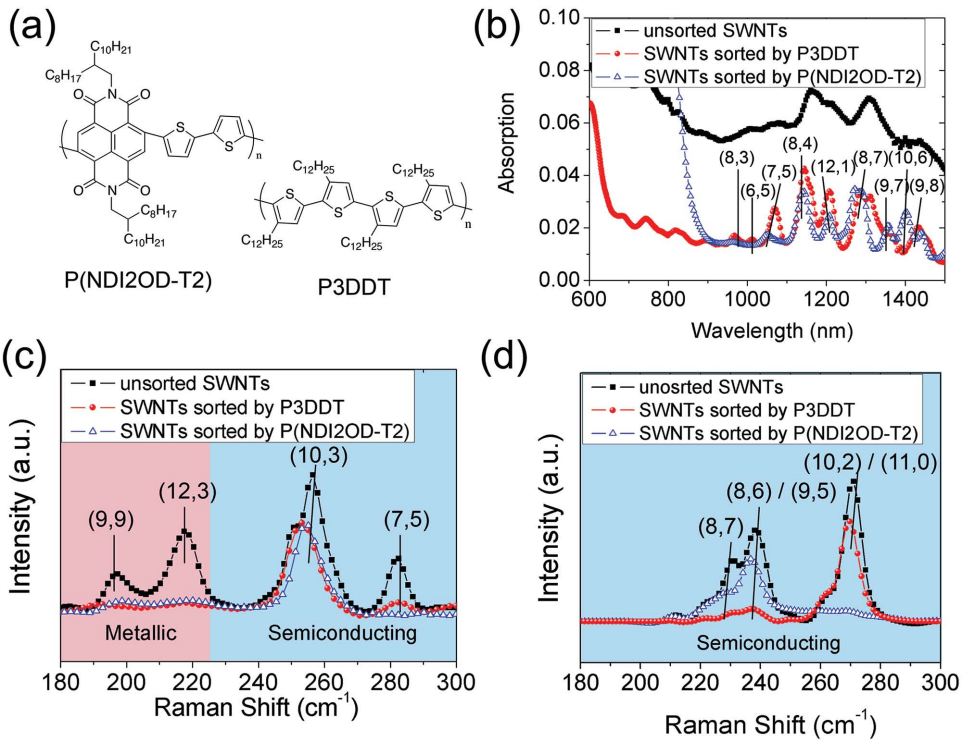

Figure 1. Characterization of P(NDI2OD-T2) sorted SWNTs. a) Polymer structure of P(NDI2OD-T2) and P3DDT. b) Optical absorbance spectra comparing unsorted SWNTs dispersed in NMP to those sorted by P3DDT and P(NDI2OD-T2) in toluene. Raman spectra of unsorted SWNTs dispersed by NMP and those dispersed by P3DDT and P(NDI2OD-T2) obtained using c) a 633 nm laser d) or a 785 nm laser.

In this work, the high-mobility n-type polymer poly([*N*,*N*′-bis(2-octyldodecyl)-naphthalene-1,4,5,8-bis(dicarboximide)-2,6-diyl]-alt-5,5′-(2,2′-bithiophene)) (P(NDI2OD-T2)) (**Figure 1**a)[17] is used for the selective dispersion of SWNTs for the first time. Surprisingly, instead of observing the expected enrichment of m-SWNTs, we achieved high-purity sorting of s-SWNTs, as characterized by Raman spectroscopy, dielectric force spectroscopy, and thin film transistors. Our selectively dispersed SWNTs by P(NDI2OD-T2) have larger diameters in comparison to those sorted by the p-type poly(3-dodecylthiophene) (P3DDT), desirable for circuit applications.[18] The observed selectivity is rationalized by molecular dynamics (MD) simulations in explicit toluene as solvent, where the atomic-scale interactions between SWNTs and the wrapping polymers can be visualized. Furthermore, using high-mobility n-type P(NDI2OD-T2) as our sorting polymer, we achieved ambipolar SWNT transistors with enhanced electron transport in comparison to P3DDT sorted SWNTs, even on flexible substrates. As a result, we demonstrated flexible complementary metal-oxide-semiconductor (CMOS)-like inverters, negated AND (NAND) and negated OR (NOR) logic circuits made from ambipolar P(NDI2OD-T2) sorted SWNT transistors. The use of P(NDI2OD-T2) polymer enables sorting of pure s-SWNTs and clear ambipolarity of SWNT transistors through a single step.

2. Result

2.1. Selecting Larger-Diameter SWNTs by P(NDI2OD-T2) Polymer

The sorting procedure was similar to our previously reported process[11] that involved mixing of SWNTs, P(NDI2OD-T2) in toluene, followed by brief sonication, centrifugation, and extraction of the supernatant. Ultraviolet–visible–near infrared (UV–vis–NIR) spectroscopy, Raman spectroscopy, and photoluminescence excitation spectroscopy (PLE) were used to characterize the chirality of SWNTs sorted by P(NDI2OD-T2) (see Section 3). The UV–vis–NIR spectrum of P(NDI2OD-T2) sorted SWNTs is shown in comparison to P3DDT-sorted SWNTs and unsorted SWNTs dispersed in N-Methyl-2-pyrrolidone (NMP) (Figure 1b). Although the overall amounts of SWNTs dispersed by the two polymers are similar, P(NDI2OD-T2) sorted SWNTs have fewer/smaller peaks at smaller wavelengths and more/higher peaks at longer wavelengths (peaks for the corresponding SWNT chirality labeled in Figure 1b), indicating successful enrichment of larger-diameter SWNTs. As shown by Raman spectroscopy (633 nm laser wavelength, Figure 1c), the P(NDI2OD-T2)-sorted SWNTs exhibited significantly less signal arising from (12,3) and (9,9) m-SWNTs, similar to our previous observations using P3DDT for sorting. In addition, P(NDI2OD-T2) selectively disperses larger-diameter (10,3) SWNTs but does not sort small-diameter (7,5) SWNTs. Using a 785 nm laser for Raman spectroscopy (Figure 1d), it is more clearly seen that P(NDI2OD-T2) enriches larger-diameter (9,5) or (8,6) s-SWNTs while P3DDT selectively disperses small-diameter (10,2) and (11,0) s-SWNTs. The enrichment of sorted large-diameter s-SWNTs by P(NDI2OD-T2) in comparison to P3DDT characterized by UV–vis–NIR and Raman spectroscopy is illustrated by the chirality map shown in **Figure 2**. We also used PLE to characterize the chiralities of P(NDI2OD-T2) sorted SWNTs as shown in Figure S1, Supporting Information.

© 2015 WILEY-VCH Verlag GmbH & Co. KGaA, Weinheim

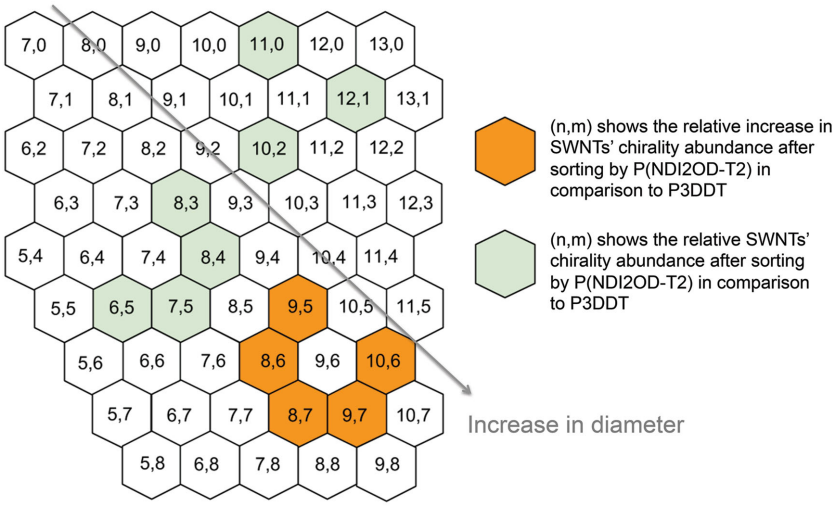

Figure 2. Chirality map showing the enrichment of SWNTs by P(NDI2OD-T2) characterized by UV–vis–NIR and Raman spectroscopy. Orange and light green hexagons correspond to an increase or decrease in the abundance of SWNTs of a specified chirality after sorting by P(NDI2OD-T2) in comparison to P3DDT, respectively.

The large-diameter SWNTs observed by Raman spectroscopy, such as (8,6), (9,5) and (10,3), are again observed by PLE. However, the strong emission at around 950 nm (likely from residual P(NDI2OD-T2)) overlaps with some small-diameter SWNT peaks such as (7,6), thereby preventing the accurate comparison of the enrichment SWNT chiralities in comparison with P3DDT-sorted SWNTs.

In order to rationalize the selective dispersion of larger-diameter SWNTs with P(NDI2OD-T2), we modeled the interaction of P(NDI2OD-T2) and P3DDT with both larger-diameter SWNTs such as (9,5) and (8,6) and the smaller-diameter SWNTs such as (10,2) and (11,0), using MD simulations. Following our previously reported methodology,[15,19] we computed the binding energies of the SWNT/polymer complexes along the MD trajectories. The binding energy (E_B) is defined as follows: $E_B = [E_{complex} - (E_{SWNT} + E_{polymer})]$, where $E_{complex}$, E_{SWNT}, and $E_{polymer}$ are the energies of the SWNT/polymer complex, the SWNT, and the polymer, respectively. Polymer strands with 32 repeating units for P3DDT (extended length: 12.5 nm) and ten repeating units for P(NDI2OD-T2) (extended length: 14.1 nm) and 30 nm long nanotubes were used in the simulations. Representative snapshots of the structures of different SWNT/polymer complexes obtained after 160 ns simulation in toluene are shown in **Figure 3** and Figures S2 and S3, Supporting Information.

We note that the MD simulations showed that P(NDI2OD-T2) adapted a more helical conformation when wrapped to small-diameter (10,2) SWNT in comparison to large-diameter (8,6) SWNT (Figure 3a,b). Since the small chiral angle (10,2) (θ = 8.9°) or (11,0) (θ = 0°) SWNTs have a more curved hexagon path along the length of SWNTs than the large chiral angle (8,6) (θ = 25.3°) or (9,5) (θ = 20.6°) SWNTs, we hypothesize that the helical wrapping of (10,2) SWNT by P(NDI2OD-T2) is a result of the polymer polycyclic aromatic backbone following the more curved hexagon path along the SWNT through well-defined π–π stacking interactions. This behavior is better represented in Figure 3c,d (colored version in Figure S2c,d, Supporting Information): the P(NDI2OD-T2) backbone closely matches the hexagon paths along both (8,6) (linear) and (10,2) (helical) SWNTs. The fused rings in the naphthalene diimide (NDI) unit are registered to interact with the SWNT in a similar way to the growth of other polycyclic aromatic compounds on a graphene surface (alternative stacking of atoms) modeled by density functional theory (DFT).[20] In the case of P3DDT, however, there is little difference in the polymer wrapping curvature when it is wrapped to both (9,5) and (11,0) SWNTs (Figure S3a,b, Supporting Information), even though these two SWNTs have rather different chiral angles and hexagon path directions as shown in Figure S3c,d, Supporting Information. The main reason preventing P3DDT to align with the hexagon path direction along the SWNT is the result of weaker π–π interactions between the less aromatic and more flexible polymer backbone composed of nonfused, five-membered thiophene rings. According to the previous work on pyrene/SWNT interactions,[21] stronger π–π interactions are expected between the 1,8-dihydropyrene-like NDI backbone core in P(NDI2OD-T2) and the SWNT surface.

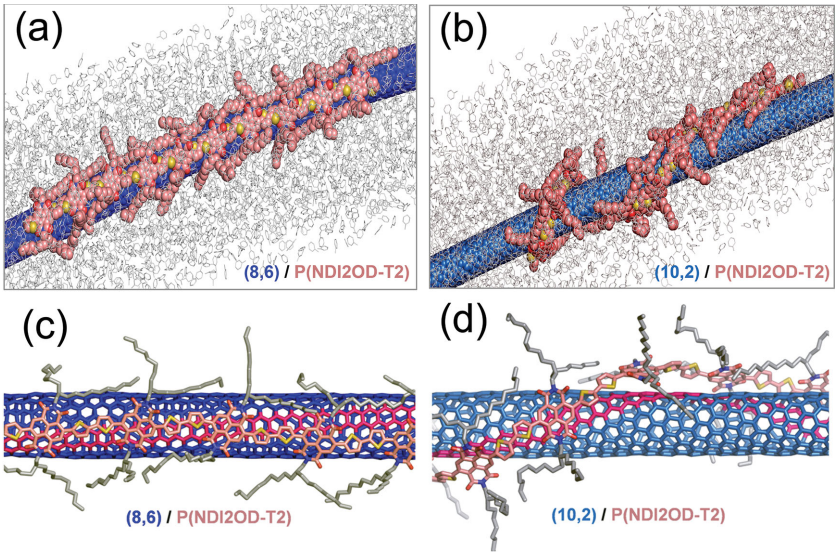

Figure 3. Representative structures of P(NDI2OD-T2) wrapping of a) large-diameter (8,6) SWNTs and b) small-diameter (10,2) SWNTs. Close-image of c) large-diameter (8,6) SWNTs and d) small-diameter (10,2). Solvent molecules have been removed for clarity. A colored version of Figure 3 showing the SWNT hexagon path and polymer structure is replotted in Figure S2, Supporting Information.

© 2015 WILEY-VCH Verlag GmbH & Co. KGaA, Weinheim

Table 1. Binding energies (E_B, kcal mol^{-1}) of eight SWNT/polymer complexes derived from 200 ns MD trajectories in explicit toluene. Binding energies are computed with 30 nm long nanotubes and polymer strands with 32 repeating units for P3DDT (extended length: 12.5 nm) and ten repeating units for P(NDI2OD-T2) (extended length: 14.1 nm).

SWNT		Polymer	
Chirality	Diameter [nm]	P(NDI2OD-T2)	P3DDT
		E_B [kcal mol^{-1}]	E_B [kcal mol^{-1}]
(8,6)	0.95	−584 ± −21	−649 ± −18
(9,5)	0.96	−584 ± −19	−650 ± −15
(10,2)	0.87	−575 ± −17	−676 ± −15
(11,0)	0.86	−572 ± −28	−677 ± −20

Interestingly, the helical binding mode in P(NDI2OD-T2)/(10,2) SWNT corresponds to the minimum dispersion of (10,2) SWNT by P(NDI2OD-T2) from our Raman spectroscopy result. The helical wrapping conformation could lead to less effective dispersion of SWNTs due to the less efficient packing between the polymer side chains in this conformation. As a consequence, the side chains establish more interactions with the solvent[15] and the binding energy with the SWNT decreases. This decrease in binding energy is supported by the calculated values as shown in **Table 1**, where the interaction is weaker between P(NDI2OD-T2) and small-diameter (10,2) or (11,0) SWNTs. In addition, this helical arrangement may also prevent additional polymer strands from wrapping onto the SWNTs surface,[22] being unable to provide enough stabilization to disperse the individual small-diameter SWNTs. On the other hand, linear wrapping between P(NDI2OD-T2) polymer and larger-diameter (9,5) and (8,6) SWNTs may allow several polymers strands to stack on the same SWNT, providing more stabilization for dispersion. Interestingly, previous simulations of poly(9,9-dioctylfluorenyl-2,7-diyl) (PFO) wrapping of SWNTs also suggested that the number of polymer strands that can be wrapped around the same SWNT increases with the SWNT diameter.[10] In addition, the more aromatic NDI core is expected to have a stronger interaction with the flatter walls of larger-diameter (9,5) and (8,6) SWNTs. Conversely, higher binding energies of P3DDT toward small-diameter SWNTs were calculated, in agreement with the observed selectivity (Table 1). This might be caused by larger-diameter SWNTs having greater surface area exposed to the solvent, which would increase their desolvation penalty prior to polymer wrapping. SWNTs with different chiralities but very similar diameters show almost identical binding energies. This result supports the observations from our previous MD simulations, which suggest that the SWNT diameter plays an important role for selective sorting, especially when both the backbone and the side chains of the polymer are tightly bound to the SWNT surface.[18]

2.2. Selective Dispersion of Semiconducting SWNTs

As discussed previously, we observed from Raman spectroscopy the suppression of m-SWNT peaks in P(NDI2OD-T2) sorted SWNTs. In order to further confirm the sorting of s-SWNTs by P(NDI2OD-T2), we used dielectric force microscopy (DFM) to characterize the fraction of s-SWNTs in the sorted samples. DFM is a simple quantitative measurement method to differentiate s-SWNTs and m-SWNTs without the need of making electrical contacts to individual SWNTs. DFM operates on the principle that s-SWNTs and m-SWNTs have different dielectric constants and therefore have different dielectric responses to external electric fields.[23] With the application of a gate bias, the charge carrier density in the s-SWNTs can be modulated but not in m-SWNTs; the change in carrier density is manifested in the dielectric response and s-SWMT/m-SWNTs can consequently be differentiated.[24] An example of how we quantify the fraction of s-SWNTs in P(NDI2OD-T2)-sorted SWNTs is demonstrated in **Figure 4**: dielectric response signal in DFM measurements of the SWNTs

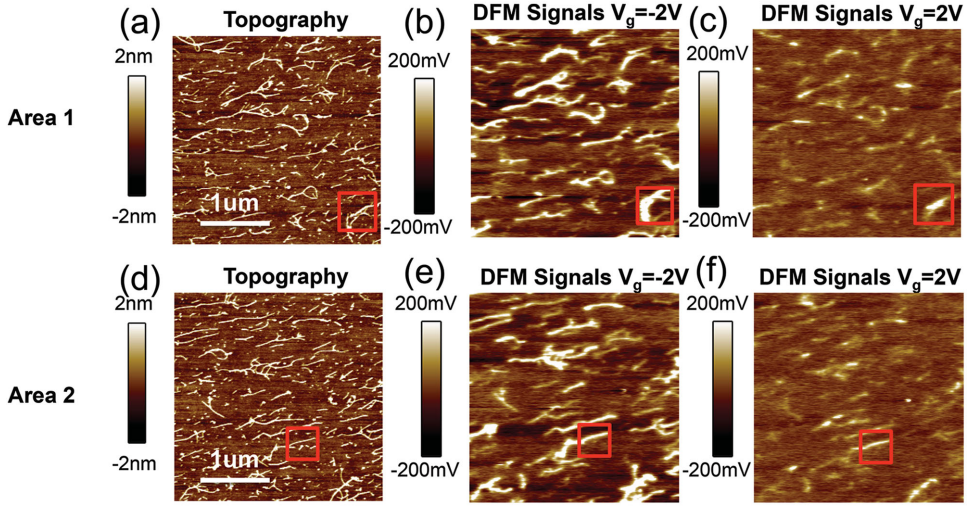

Figure 4. Representative images showing the dielectric force measurements to determine the ratios of s-SWNT to m-SWNTs. a,d) Topography of SWNTs. b,e) Dielectric response signal of the SWNTs measured with DFM under a gate bias voltage of −2 V. c,f) Dielectric response signal of the SWNTs measured with DFM under a gate bias voltage of 2 V.

© 2015 WILEY-VCH Verlag GmbH & Co. KGaA, Weinheim

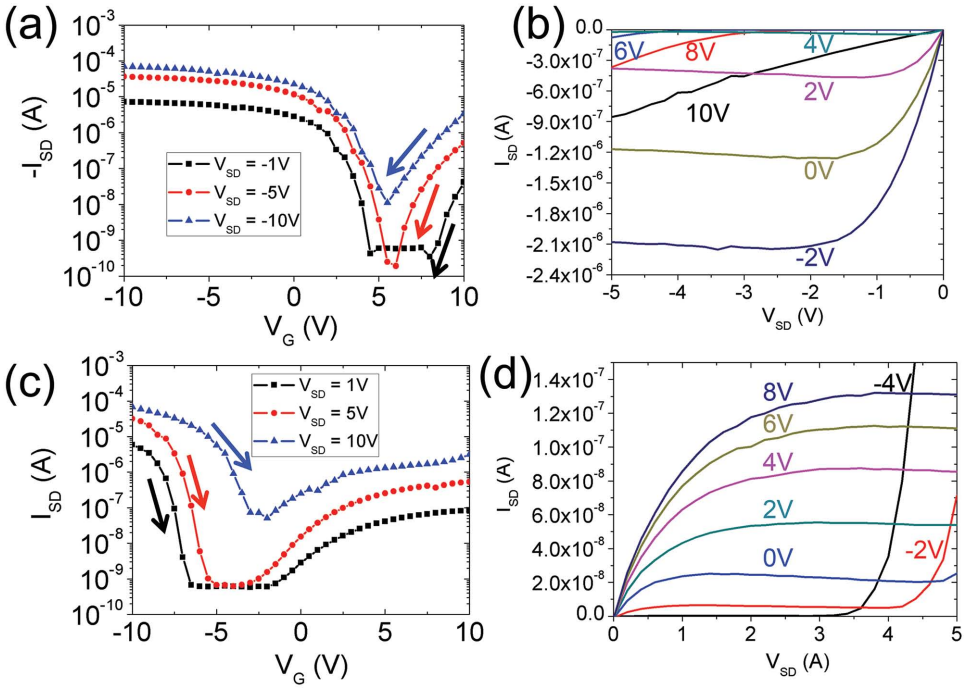

Figure 5. Flexible ambipolar transistor based on P(NDI2OD-T2) sorted SWNTs. a) Transfer characteristics at negative source–drain voltage for p-type sweep and b) their output characteristics. c) Transfer characteristics at positive source–drain voltage for n-type sweep and d) their output characteristics.

represents their charge charier density under external gate voltages. The SWNTs in the two squared areas did not show much change in intensity between positive and negative gate voltages; hence, these two SWNTs are metallic. The rest of SWNTs in the images all showed significantly decreased DFM signal as the gate bias changed from −2 to 2 V, indicating that they are semiconducting.[34] Close-up images showing the difference of metallic and semiconducting SWNTs in response to gate voltages are shown in Figure S4, Supporting Information. With P(NDI2OD-T2)-sorted SWNT samples, we measured 533 individual SWNTs and found that 528, or 99.1%, of them were semiconducting. For comparison, we also analyzed the P3DDT-sorted SWNTs found that 703 of 726, or 96.8%, of the SWNTs were semiconducting. Hence, this shows that P(NDI2OD-T2)-sorted s-SWNTs are at least as pure as the P3DDT-sorted SWNTs. In addition, we fabricated over 20 SWNT thin film transistors (L = 20 µm, W = 400 µm) based on P(NDI2OD-T2)-sorted SWNTs and their average on/off ratio was as high as $7.3 \times 10^5 \pm 6.7 \times 10^5$ with an average mobility of 0.58 ± 0.28 $cm^2\ V^{-1}\ s^{-1}$. A device with mobility of 1.2 $cm^2\ V^{-1}\ s^{-1}$ and on/off ratio of over 10^6 is shown in Figure S5a, Supporting Information (with an atomic force microscopy (AFM) image showing the very high density of the SWNT film shown in Figure S5b, Supporting Information). The robust operation of these high-density polymer-sorted SWNT devices supports that P(NDI2OD-T2) is effective for sorting s-SWNTs. From all these characterization techniques, we can conclude that both electron-donating and electron-accepting conjugated polymers can be used to sort high-purity s-SWNTs.

2.3. Ambipolar Devices for Flexible CMOS-Like Circuits

We also fabricated transistors based on P(NDI2OD-T2)-sorted SWNTs by spin-coating and measured their characteristics in an inert N_2 atmosphere (Figure S6, Supporting Information). Notably, we observed clear ambipolar behavior of P(NDI2OD-T2)-sorted SWNTs in comparison to primarily p-type P3DDT-sorted SWNTs measured under the same conditions. Three factors might contribute to this observation: (1) the n-type P(NDI2OD-T2) itself enhances the electron current of the devices. (2) P(NDI2OD-T2) modifies the Schottky barrier height between the SWNTs and metal electrodes to improve the electron injection in the device. (3) P(NDI2OD-T2) passivates the electron traps better than P3DDT at the oxide surface. The exact reason is the subject of our future investigation.

On successfully fabricating both the ambipolar transistors from P(NDI2OD-T2)-sorted SWNTs, we fabricated devices on flexible polyimide substrates (fabrication methods in the Supporting Information) and characterized their electrical behavior in an inert N_2 atmosphere. By using both p-type sweep (defined from 10 to −10 V at negative source–drain voltage, shown in **Figure 5**a) and n-type sweep (defined from −10 to 10 V at positive source–drain voltage, shown in Figure 5c), we again observed clear ambipolar characteristics in both scenarios. The off-regime voltage period is longer when lower source–drain voltage is used, a result of reduced band bending for charge injection. The output characteristics for the flexible devices are shown in Figure 5b,d, and demonstrate the typical ambipolar characteristics of the curves. Taking advantage of the

© 2015 WILEY-VCH Verlag GmbH & Co. KGaA, Weinheim

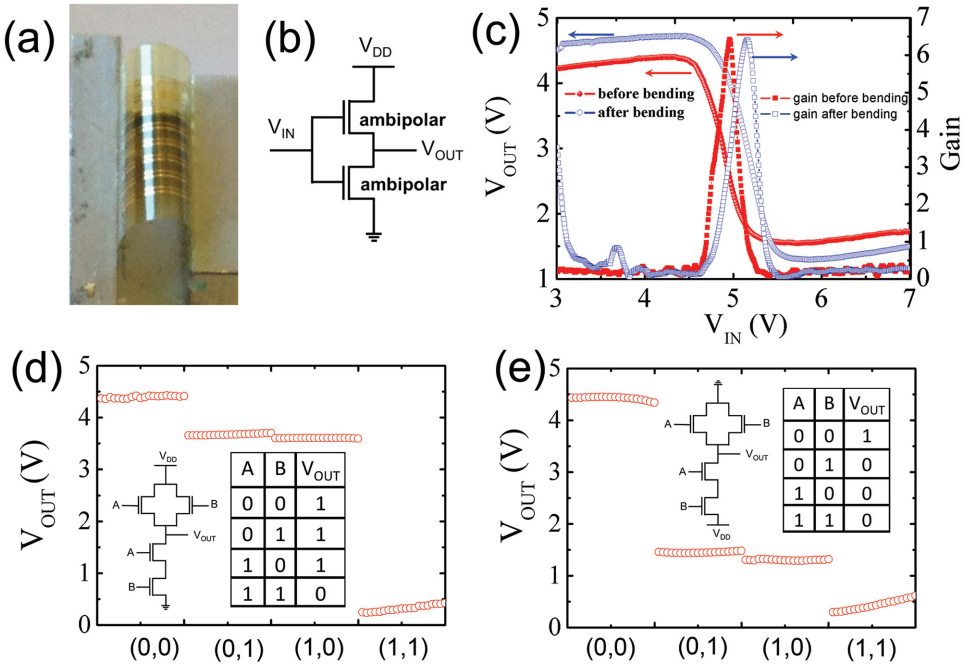

Figure 6. Application of ambipolar transistor in CMOS-like logic circuits. a) A digital photograph showing bending of flexible inverters and logic gates. b) Circuit diagram for CMOS-like inverter. c) Flexible CMOS-like inverters before and after bending. Output characteristics, circuit diagram, and truth tables for flexible CMOS-like d) NAND and e) NOR logic gates at V_{DD} = 5 V.

ambipolar nature of the devices, we fabricated CMOS-like inverters, NAND and NOR logic gates on the flexible substrate (**Figure 6**a) without separately patterning p-type of n-type regimes. Since the CMOS-like inverter only needs ambipolar SWNT transistors, only one layer of semiconducting material is needed (Figure 6b). Upon bending to a radius of curvature of 2 mm, the inverter can operate with a similar gain (≈6) as an unbent inverter, with an even higher voltage swing (Figure 6c). This increase in voltage swing was also observed in previously reported SWNT logic gates after bending process.[25] For NAND and NOR logic gates, two transistors are in series and another two transistors in parallel. With these ambipolar transistors, the same set of four transistors can act as both NAND gate and NOR gate (circuits diagram and truth tables shown in Figure 6d,e). The only change is to swap the V_{DD} and ground voltage to realize the function of either logic gate. The logic gates demonstrate excellent performance with distinct "1" or "0" voltage levels and reasonably high voltage swings (Figure 6d,e). The main limitation of CMOS-like circuit is that the ambipolar nature of the transistors prevents them from achieving full voltage swings.

3. Conclusion

In summary, we developed the first example of utilizing n-type conjugated polymers for selectively dispersing s-SWNTs. The enrichment in s-SWNTs was characterized by Raman spectroscopy, dielectric force microscopy, and thin film transistor measurements. In contrast to P3DDT, we found that P(NDI2OD-T2) selectively dispersed larger-diameter SWNTs. MD simulations showed the distinct geometry of P(NDI2OD-T2) when wrapping different types of SWNTs in comparison to P3DDT, likely due to the stronger registration between its aromatic backbone and the hexagon path of SWNTs. This distinct wrapping geometry of P(NDI2OD-T2) might result in its preferred interaction with larger-diameter, more planar SWNTs. Furthermore, we found that P(NDI2OD-T2)-sorted SWNT transistors demonstrate clear ambipolar transport behavior, which can be exploited to fabricate CMOS-like inverters, NAND and NOR logic gates on the flexible substrate. The use of P(NDI2OD-T2) for sorting s-SWNTs as well as using the resulting ambipolar SWNT transistors for CMOS-like logic circuits greatly simplifies the fabrication of flexible SWNT logic circuits.

4. Experimental Section

Preparation of SWNT Solutions: Procedures were similar to those used in our previously published report.[11] 4 mg of HiPco SWNTs purchased from Unidym and 5 mg P(NDI2OD-T2) purchased from Polyera Corporation were mixed in 25 mL of toluene and sonicated in a Cole Parmer probe sonicator (750 W) at 70% amplitude for 30 min cooled with an acetone/dry ice bath. The solution was then subjected to centrifuged (Sorvall RC5C-plus) at 17 000 rpm for 1 h. Finally, the supernatant was collected and used without further processing.

SWNT Characterization: Tapping mode AFM images were obtained using Veeco AFM. Raman spectra were obtained using a confocal Raman system (LabRam Aramis from Horiba Jobin Yvon) using 633 nm (1.96 eV) and 785 nm (1.58 eV) as the excitation laser wavelengths. Data were processed by averaging nine points over different areas in the sample, with each point obtained as an average of three spectra and calibrated to the 521 cm^{-1} silicon peak. The UV–vis–NIR measurements were obtained on Cary 6000i spectrophotometer (Varian) using a quartz cell. PLE measurements were performed on a Nanolog spectrofluorometer (Horiba Jobin Yvon).[11]

© 2015 WILEY-VCH Verlag GmbH & Co. KGaA, Weinheim

MD Simulations: The simulations were performed by using AMBER 12[26] and the general AMBER force field (GAFF).[27] 30 nm long nanotubes and polymers with 32 repeating units for P3DDT and ten repeating units for P(NDI2OD-T2) were employed in each simulation. 100 ns simulations were first performed in implicit solvent for the initial wrapping process. Subsequently, 200 ns simulations were performed in explicit solvent by immersing each wrapped polymer/SWNT complex in a pre-equilibrated bath (cubic box) of toluene molecules[28] with an internal offset distance of 20 Å, using the leap module,[29] which resulted in the addition of around 7000 solvent molecules. Given the structural differences between the different types of polymers and nanotubes considered, and in order to better estimate the binding energies of each pair, independent trajectories were run for each separated component, in addition to the polymer/SWNT complexes. For a thorough description of the procedures and general methods used in the simulations, see our previous work.[19]

Transistor Fabrication and Characterization: The drain/source electrodes for bottom-contact devices were fabricated by standard photolithography and metal evaporation (5 nm Cr and 40 nm Au).[13] The substrates were then soaked in dilute solutions of P(NDI2OD-T2)-sorted SWNTs (1:10 dilution ratio) in toluene for 8 h. A Keithley 4200 SC semiconductor analyzer was used for measuring device characteristics.

Fabrication of Flexible Transistors and Circuits: The fabrication procedures for flexible devices and circuits was reported in our previous work.[3] Polyimide solution (HD MicroSystems) was spin-cast on a silicon wafer and annealed up to 350 °C.[30] A patterned gate electrode consisting of 40 nm Au and 5 nm Ti was then patterned. Atomic layer deposition (ALD) deposited Al_2O_3 at 150 °C was used as the dielectric. Then 5 nm Ti and 40 nm Au were deposited as source/drain electrodes by standard photolithography process. The device was then soaked in P(NDI2OD-T2)-dispersed s-SWNTs at dilution ratio of 1:10 in toluene for 14 h.

Supporting Information

Supporting Information is available from the Wiley Online Library or from the author.

Acknowledgements

This work was funded by National Science Foundation (Z.B. Award No. 1059020; K.N.H.: CHE-1361104) and the Global Climate and Energy Project (GCEP) at Stanford University. We also thank Jeremy Feldblyum and Anthony Appleton for helpful discussions. H.W. acknowledges financial support from Link foundation Energy fellowship. Y.C.L. thanks his supporting funding from Taiwan National Science Council (102-2917-i-002-087). L.C. thanks the funding support from National Natural Science Foundation of China (No. 91233104) and Jiangsu Provincial Natural Science Foundation (No. BK20130006).

Received: November 21, 2014
Revised: December 21, 2014
Published online: February 13, 2015

[1] a) T. Dürkop, S. A. Getty, E. Cobas, M. S. Fuhrer, *Nano Lett.* **2003**, *4*, 35; b) H. Wang, J. Luo, A. Robertson, Y. Ito, W. Yan, V. Lang, M. Zaka, F. Schäffel, M. H. Rümmeli, G. A. D. Briggs, J. H. Warner, *ACS Nano* **2010**, *4*, 6659; c) P. Avouris, Z. Chen, V. Perebeinos, *Nat. Nanotechnol.* **2007**, *2*, 605; d) G. S. Tulevski, A. D. Franklin, D. Frank, J. M. Lobez, Q. Cao, H. Park, A. Afzali, S.-J. Han, J. B. Hannon, W. Haensch, *ACS Nano* **2014**, *8*, 8730.

[2] a) S. Park, M. Vosguerichian, Z. Bao, *Nanoscale* **2013**, *5*, 1727; b) D. J. Lipomi, M. Vosgueritchian, B. C. K. Tee, S. L. Hellstrom, J. A. Lee, C. H. Fox, Z. Bao, *Nat. Nanotechnol.* **2011**, *6*, 788.

[3] H. Wang, P. Wei, Y. Li, J. Han, H. R. Lee, B. D. Naab, N. Liu, C. Wang, E. Adijanto, B. C.-K. Tee, S. Morishita, Q. Li, Y. Gao, Y. Cui, Z. Bao, *Proc. Natl. Acad. Sci. U.S.A.* **2014**, *111*, 4776.

[4] a) P. H. Lau, K. Takei, C. Wang, Y. Ju, J. Kim, Z. Yu, T. Takahashi, G. Cho, A. Javey, *Nano Lett.* **2013**, *13*, 3864; b) M. Ha, Y. Xia, A. A. Green, W. Zhang, M. J. Renn, C. H. Kim, M. C. Hersam, C. D. Frisbie, *ACS Nano* **2010**, *4*, 4388; c) L. Hu, D. S. Hecht, G. Grüner, *Chem. Rev.* **2010**, *110*, 5790.

[5] M. S. Arnold, A. A. Green, J. F. Hulvat, S. I. Stupp, M. C. Hersam, *Nat. Nanotechnol.* **2006**, *1*, 60.

[6] X. Tu, S. Manohar, A. Jagota, M. Zheng, *Nature* **2009**, *460*, 250.

[7] H. Liu, D. Nishide, T. Tanaka, H. Kataura, *Nat. Commun.* **2011**, *2*, 309.

[8] C. Y. Khripin, J. A. Fagan, M. Zheng, *J. Am. Chem. Soc.* **2013**, *135*, 6822.

[9] S. K. Samanta, M. Fritsch, U. Scherf, W. Gomulya, S. Z. Bisri, M. A. Loi, *Acc. Chem. Res.* **2014**, *47*, 2446.

[10] A. Nish, J. Y. Hwang, J. Doig, R. J. Nicholas, *Nat. Nanotechnol.* **2007**, *2*, 640.

[11] H. W. Lee, Y. Yoon, S. Park, J. H. Oh, S. Hong, L. S. Liyanage, H. Wang, S. Morishita, N. Patil, Y. J. Park, J. J. Park, A. Spakowitz, G. Galli, F. Gygi, P. H. S. Wong, J. B. H. Tok, J. M. Kim, Z. Bao, *Nat. Commun.* **2011**, *2*, 541.

[12] a) S. Park, H. W. Lee, H. Wang, S. Selvarasah, M. R. Dokmeci, Y. J. Park, S. N. Cha, J. M. Kim, Z. Bao, *ACS Nano* **2012**, *6*, 2487; b) H. Wang, G. I. Koleilat, P. Liu, G. Jiménez-Osés, Y.-C. Lai, M. Vosgueritchian, Y. Fang, S. Park, K. N. Houk, Z. Bao, *ACS Nano* **2014**, *8*, 2609.

[13] H. Wang, J. Mei, P. Liu, K. Schmidt, G. Jiménez-Osés, S. Osuna, L. Fang, C. J. Tassone, A. P. Zoombelt, A. N. Sokolov, K. N. Houk, M. F. Toney, Z. Bao, *ACS Nano* **2013**, *7*, 2659.

[14] a) J.-Y. Hwang, A. Nish, J. Doig, S. Douven, C.-W. Chen, L.-C. Chen, R. J. Nicholas, *J. Am. Chem. Soc.* **2008**, *130*, 3543; b) K. S. Mistry, B. A. Larsen, J. L. Blackburn, *ACS Nano* **2013**, *7*, 2231; c) W. Gomulya, G. D. Costanzo, E. J. F. De Carvalho, S. Z. Bisri, V. Derenskyi, M. Fritsch, N. Fröhlich, S. Allard, P. Gordiichuk, A. Herrmann, S. J. Marrink, M. C. Dos Santos, U. Scherf, M. A. Loi, *Adv. Mater.* **2013**, *25*, 2948; d) W. Z. Wang, W. F. Li, X. Y. Pan, C. M. Li, L.-J. Li, Y. G. Mu, J. A. Rogers, M. B. Chan-Park, *Adv. Funct. Mater.* **2011**, *21*, 1643; e) T. Fukumaru, F. Toshimitsu, T. Fujigaya, N. Nakashima, *Nanoscale* **2014**, *6*, 5879; f) N. Berton, F. Lemasson, A. Poschlad, V. Meded, F. Tristram, W. Wenzel, F. Hennrich, M. M. Kappes, M. Mayor, *Small* **2014**, *10*, 360.

[15] H. Wang, B. Hsieh, G. Jiménez-Osés, P. Liu, C. J. Tassone, Y. Diao, T. Lei, K. N. Houk, Z. Bao, *Small* **2015**, *11*, 126.

[16] a) H.-J. Shin, S. M. Kim, S.-M. Yoon, A. Benayad, K. K. Kim, S. J. Kim, H. K. Park, J.-Y. Choi, Y. H. Lee, *J. Am. Chem. Soc.* **2008**, *130*, 2062; b) N. Varghese, A. Ghosh, R. Voggu, S. Ghosh, C. N. R. Rao, *J. Phys. Chem. C* **2009**, *113*, 16855.

[17] H. Yan, Z. Chen, Y. Zheng, C. Newman, J. R. Quinn, F. Dotz, M. Kastler, A. Facchetti, *Nature* **2009**, *457*, 679.

[18] a) X. Zhou, J.-Y. Park, S. Huang, J. Liu, P. L. McEuen, *Phys. Rev. Lett.* **2005**, *95*, 146805; b) Z. Chen, J. Appenzeller, J. Knoch, Y.-M. Lin, P. Avouris, *Nano Lett.* **2005**, *5*, 1497.

[19] H. Wang, G. I. Koleilat, P. Liu, G. Jiménez-Osés, Y.-C. Lai, M. Vosgueritchian, Y. Fang, S. Park, K. N. Houk, Z. Bao, *ACS Nano* **2014**, *8*, 2609.

[20] a) X. Q. Tian, J. B. Xu, X. M. Wang, *J. Phys. Chem. C* **2010**, *114*, 20917; b) S. M. Kozlov, F. Viñes, A. Görling, *Adv. Mater.* **2011**, *23*, 2638.

[21] a) R. J. Chen, S. Bangsaruntip, K. A. Drouvalakis, N. W. S. Kam, M. Shim, Y. Li, W. Kim, P. J. Utz, H. Dai, *Proc. Natl. Acad. Sci. U.S.A.* **2003**, *100*, 4984; b) K. C. Etika, F. D. Jochum, P. Theato, J. C. Grunlan, *J. Am. Chem. Soc.* **2009**, *131*, 13598.

© 2015 WILEY-VCH Verlag GmbH & Co. KGaA, Weinheim

[22] M. Bernardi, M. Giulianini, J. C. Grossman, *ACS Nano* **2010**, *4*, 6599.
[23] W. Lu, D. Wang, L. Chen, *Nano Lett.* **2007**, *7*, 2729; b) W. Lu, Y. Xiong, A. Hassanien, W. Zhao, M. Zheng, L. Chen, *Nano Lett.* **2009**, *9*, 1668.
[24] a) W. Lu, J. Zhang, Y. S. Li, Q. Chen, X. Wang, A. Hassanien, L. Chen, *J. Phys. Chem. C* **2012**, *116*, 7158; b) Y. Li, J. Ge, J. Cai, J. Zhang, W. Lu, J. Liu, L. Chen, *Nano Res.* **2014**, *7*,1623.
[25] Y. Ando, X. Zhao, T. Sugai, M. Kumar, *Mater. Today* **2004**, *7*, 22.
[26] A. D. Case, T. A. Darden, T. E. Cheatham III, C. L. Simmerling, J. Wang, R. E. Duke, R. Luo, R. C. Walker, W. Zhang, K. M. Merz, B. Roberts, S. Hayik, A. Roitberg, G. Seabra, J. Swails, A. W. Goetz, I. Kolossváry, K. F. Wong, F. Paesani, J. Vanicek, R. M. Wolf, J. Liu, X. Wu, S. R. Brozell, T. Steinbrecher, H. Gohlke, Q. Cai, X. Ye, J. Wang, M.-J. Hsieh, G. Cui, D. R. Roe, D. H. Mathews, M. G. Seetin, R. Salomon-Ferrer, C. Sagui, V. Babin, T. Luchko, S. Gusarov, A. Kovalenko, P. A. Kollman, AMBER 12, **2012**.
[27] J. Wang, R. M. Wolf, J. W. Caldwell, P. A. Kollman, D. A. Case, *J. Comput. Chem.* **2004**, *25*, 1157.
[28] C. M. Baker, G. H. Grant, *J. Chem. Theory Comput.* **2007**, *3*, 530.
[29] C. E. A. F. Schafmeister, W. F. Ross, V. Romanovsky, University of California, San Francisco **1995**.
[30] A. J. Kronemeijer, E. Gili, M. Shahid, J. Rivnay, A. Salleo, M. Heeney, H. Sirringhaus, *Adv. Mater.* **2012**, *24*, 1558.

© 2015 WILEY-VCH Verlag GmbH & Co. KGaA, Weinheim